Experimental and modeling study of the effect of ethanol and MTBE on the oxidation of PRF90 in low pressure premixed laminar flame

ARTICLE *in* FUEL · SEPTEMBER 2013

Impact Factor: 3.52 · DOI: 10.1016/j.fuel.2013.04.038

3 AUTHORS, INCLUDING:

Chunde Yao
Tianjin University
138 PUBLICATIONS **768** CITATIONS
SEE PROFILE

Guanglan Xu
Tianjin University
9 PUBLICATIONS **47** CITATIONS
SEE PROFILE

Fuel 111 (2013) 131–139

Contents lists available at SciVerse ScienceDirect

Fuel

journal homepage: www.elsevier.com/locate/fuel

Experimental and modeling study of the effect of ethanol and MTBE on the oxidation of PRF90 in low pressure premixed laminar flame

Chunde Yao *, Guanglan Xu, Hanjun Xu

State Key Laboratory of Engines, Tianjin University, Tianjin 300072, China

HIGHLIGHTS

- Low-pressure laminar premixed flames of PRF90/ethanol and PRF90/MTBE were realized.
- A detailed mechanism for the low-pressure oxidation of the blends was developed.
- The effect of ethanol and MTBE on high temperature oxidation of PRF90 was analyzed.

ARTICLE INFO

Article history:
Received 6 July 2012
Received in revised form 8 March 2013
Accepted 16 April 2013
Available online 3 May 2013

Keywords:
Ethanol
MTBE
Gasoline
Primary reference fuel
Premixed laminar flame

ABSTRACT

Two premixed laminar flames of PRF90 (Primary Reference Fuel, iso-octane:*n*-heptane is 9:1) blended with ethanol and MTBE (Methyl Tert-Butyl Ether) respectively were studied, using molecular-beam sampling technology combining with tunable synchrotron VUV (Vacuum Ultra-Violet) photoionization mass spectrometry. Mole fraction profiles of species including reactants, intermediates and products were derived from the measurement. A detailed mechanism for high temperature oxidation under low pressure of the fuels mentioned above was developed based on USC-Mech II and each fuel sub-mechanism. The modeling result shows that the radical pool is affected by the change of additives and this leads to a slight change of PRF (Primary Reference Fuel) consumption paths. Both experimental and modeling results show that species with carbon number more than four and species with high unsaturation degree are not affected by the change of additives, while alkadienes are a little higher and acetaldehyde is lower in PRF90/MTBE flame, comparing with those in the PRF90/ethanol flame. In addition, the experimental result shows methanol and other carbonyl compounds including formaldehyde, acetone and butanone have higher concentrations in PRF90/MTBE flame.

1. Introduction

Gasoline is a wide used petrol fuel in the world. Some oxygenated additives are selected as octane enhancer to reduce its knock tendency. MTBE (Methyl Tert-Butyl Ether) was authorized by the United States for use as an anti-knock additive in 1979 [1] because of its advanced physical and chemical properties in combustion. However, it has been reported that MTBE will pollute the underground water [2,3]. Therefore, the use of MTBE is reduced from its former scale in recent years and is replaced by ethanol or other oxygenated additives that are less harmful to the environment. Ethanol is increasingly used in the United States and other developed countries [4–6]. But MTBE will still be used in developing countries such as China, which has a large population but is lack of plowland, besides adequate evidence of health risk of MTBE is still lack so far. So, ethanol and MTBE are the most widely used oxygenated additives to improve motor vehicle fuel properties around the world now and will last for a long time. Therefore, the impact of ethanol and MTBE additives on gasoline combustion has attracted much concern.

Most of the researches about ethanol and MTBE additives are concerned on their impacts to engine exhaust emissions. Ethanol and MTBE can both reduce emissions of unburned hydrocarbons and carbon monoxide but increase emissions of nitrogen oxides and ethanol also causes an increase in acetaldehyde [4–11]. Comparison work of effects of ethanol and MTBE addition into gasoline on exhaust emission was done by Song et al. [12]. Their results show that overall ethanol has a better performance than MTBE on the regular emissions, while MTBE has advantages in benzene and acetaldehyde emission reduction. Chemical kinetic and flame studies of ethanol and MTBE were also conducted by many researchers to understand their oxidation and co-oxidation with hydrocarbon fuel. For instance, the oxidation behaviors of ethanol and MTBE were investigated by using premixed flame, diffusion flame and jet-stirred reactor [13–16]. The co-oxidation of multi

* Corresponding author. Tel.: +86 22 2740 6649; fax: +86 22 2738 3362.
E-mail address: arcdyao@tju.edu.cn (C. Yao).

0016-2361/$ - see front matter © 2013 Elsevier Ltd. All rights reserved.
http://dx.doi.org/10.1016/j.fuel.2013.04.038

compound fuels with quite different chemical and physical properties is favored by many researchers recently. Dagaut and Togbé [17] investigated the oxidation of ethanol/*n*-heptane mixtures in a jet-stirred reactor to detect the intermediate and to test the multi fuels reaction mechanism. Haas et al. [18] investigated ethanol and ethanol/PRF (Primary Reference Fuel) blends oxidations in low and intermediate temperature. The role of radical pool connecting different fuels is confirmed in their work. However, the effect of high-temperature oxidation behavior which refers to the flame structure and combustion just comes into concern. Song et al. [19,20] investigated the effects of ethanol and MTBE on *n*-heptane oxidation in premixed laminar flame by using tunable synchrotron VUV (Vacuum Ultra-Violet) photoionization. It is deduced from species detection that reaction paths of some intermediates change with the change of additives. However, quantitative kinetic analysis and branch alkane fuels were not involved. Yao et al. [21,22] compared the effects of ethanol and MTBE addition to commercial gasoline using the same device as Song et al. [19,20]. Toxic emission evolution was their major concern and no chemical kinetic study was conducted, because gasoline is a complex mixture of hydrocarbon constituents and the interactions among the chemical constituents are not fully understood.

In this study, PRF90 (the ratio of iso-octane/*n*-heptane is 9:1 by volume in liquid) is used as gasoline surrogate in both experiment and modeling. Specific emphasis is given to the kinetic comparison of effects of ethanol and MTBE on the high temperature oxidation of hydrocarbons. Premixed laminar flame combining with molecular beam sampling technology is used to detect relatively stable species at different positions. Accurate measurement of species is conducted by using the tunable synchrotron VUV photoionization mass spectrometry. A detailed high temperature oxidation mechanism involving the sub-mechanisms of each fuel under low pressure was developed for the modeling. Kinetic analysis was conducted to seek the couple relationship between the fuels and the oxidation property of each individual.

2. Experiment

The flame experiment was conducted at the Combustion and Flame Endstation of the National Synchrotron Radiation Laboratory in the University of Science and Technology of China. The instruments have been reported in previous literature [23–25], a brief description is given here. It is the flame-sampling molecular-beam mass spectrometry of premixed, laminar, low-pressure flat flame combining with synchrotron VUV radiation as the photoionization light source. The system contains a Mckenna burner with a diameter of 6 cm, a sample nozzle made of quartz, a time of flight mass spectrometer and three chambers including the flame chamber, first stage expansion region and second stage expansion region (ionization chamber). The pressure is about 10–100 torr at the first chamber and decreases to 10^{-6} torr at the last chamber. The molecular beam from the quartz sampling nozzle crosses with the light from the synchrotron and then the molecule is ionized. Then the ion is introduced into a mass spectrometer for their separation by weight. This photoionization is just "soft ionization", so it has high resolution and precision because fragmentation can be avoided.

Flame conditions are listed in Table 1. The pressure is 25 torr in the flame chamber. The blending ratio of PRF90/additive is 9:1 (by volume in liquid) and it has been reported that the two mixtures have almost the same octane number of 94.7 [12]. PRF90/ethanol and PRF90/MTBE blends are marked as Flame E and Flame M respectively. The equivalence ratio was kept at stoichiometric ratio and the C/O ratio was kept around 0.32 for both flames. Two vaporizers are used in the vaporization of fuel sample. One is prepared for PRF90 which is premade because the boiling points of iso-octane and *n*-heptane are very close (99.3 °C and 98.4 °C respectively under atmosphere). Another vaporizer is for the additive which has lower boiling point than PRF (78.4 °C for ethanol and 55.2 °C for MTBE under atmosphere). The flame flickering caused by unstable vaporizer and the flow rate can be avoided by the separate vaporization.

The photon energy used in this study is 9.0, 9.5, 10.0, 11.0, 11.8, 13.19, 14.6, and 16.53 eV. The minimal step for the burner scan is 0.5 mm. Mole fractions of flame species were derived based on the method described by Cool et al. [26,27]. Photoionization cross sections (PICSs) are taken from website [28], the cross section values for the intermediates with unknown PICSs are estimated using methods [29]. The uncertainties of evaluated mole fractions are about ±10% for major species, ±25% for intermediates with known PICSs, and a factor of 2 for those with estimated PICSs. The flame temperature is measured by using a 0.1-mm-diameter Pt–6%Rh/Pt–30%Rh thermocouple coated with Y_2O_3–BeO anti-catalytic ceramic [30], and is corrected for the radiation heat loss [31] and cooling effects of sampling nozzle [32]. The experimental error of the maximum flame temperature is estimated to be ±100 K. The effect of the temperature deviation on the modeling results for Flame E are shown in Figs. S1 and S2 in Supplemental material. Overall, the uncertainty in the temperature mainly induces the error of the position prediction of mole fraction profiles but results in tiny influence of the shape of mole fraction profiles.

3. Reaction mechanism

The USC-Mech II was used as C1–C4 basic mechanism. All the four fuels have their detailed reaction mechanisms. However, the fall-off effect under low pressure was not considered for some pressure-dependent elementary. Thus, pressure correction was conducted for those reactions. At the same time, reactions relating to mutual coupling effects between the fuel molecules were examined. The reaction mechanism of ethanol is relatively mature, covering various pressure ranges. The ethanol oxidation mechanism developed by Li [33] with some reactions revised according to a previous study [34], and the MTBE mechanism included in the general ether mechanism developed by Curran et al. [35] were used in this study. The effect of the pressure was considered for the fuel direct decomposition elementary reactions, while not for the fuel radical decomposition reactions. Therefore, the rate coefficients of these pressure-dependent reactions were estimated

Table 1
Experimental conditions of PRF90/ethanol and PRF90/MTBE premixed laminar flames in low pressure.

	$X_{\text{iso-octane}}$ (%)	$X_{n\text{-heptane}}$ (%)	X_{ethanol} (%)	X_{MTBE} (%)	X_{O_2} (%)	X_{Ar} (%)	Mass flow rate (g/(s cm^2))
Flame E[a]	4.174	0.523	1.456	–	61.858	31.989	0.002535
Flame M[b]	4.153	0.520	–	0.711	62.624	31.992	0.002547

X: mole fraction of species.
[a] Flame with ethanol addition.
[b] Flame with MTBE addition.

Table 2
Pressure dependent reactions of iso-octane.

Reactions	Rate coefficients (cm-mol-s-kcal) ($k = AT^{**}b\ \exp(-E/RT)$)				Ref.[a]
	A	b	E		
$aC_8H_{17} + H(+M) = iC_8H_{18}(+M)$	3.60E+13	0.00	0.0		A
	LOW/3.27E+56	−11.74	6430.8/		
	TROE/0.506	1266.6	1266.6	50000.0/	
	2.40E+13	0.00	0.0		
$bC_8H_{17} + H(+M) = iC_8H_{18}(+M)$	LOW/1.70E+58	−12.08	11263.7/		B
	TROE/0.649	1213.1	1213.1	13369.7/	
	2.40E+13	0.00	0.0		
$cC_8H_{17} + H(+M) = iC_8H_{18}(+M)$	LOW/1.47E+61	−12.94	8000.0/		C
	TROE/0.000	1456.4	1000.0	10000.5/	
	1.60E+13	0.00	0.0		
$dC_8H_{17} + H(+M) = iC_8H_{18}(+M)$	LOW/2.18E+56	−11.74	6430.8/		A(2/3)
	TROE/0.506	1266.6	1266.6	50000.0/	
	3.57E+11	0.65	30856.0		
$aC_8H_{17}(+M) = xC_7H_{14} + CH_3(+M)$	LOW/1.05E+58	−12.85	35567.0/		D(1/6)
	TROE/0.986	−300	1	1E30/	
$aC_8H_{17}(+M) = iC_4H_8 + iC_4H_9(+M)$					
$nC_7H_{15}(+M) = iC_4H_8 + nC_3H_7(+M)$	1.325E+13	0.0	27828.0		
$hC_6H_{13}(+M) = C_2H_4 + tC_4H_9(+M)$	LOW/2.371E+55	−11.91	32263.0/		E(5/4)
$cC_8H_{17}(+M) = iC_4H_8 + tC_4H_9(+M)$	TROE/0.987	−219.1	1	1E30/	
$pC_7H_{15}(+M) = tC_4H_9 + C_3H_6(+M)$					
	5.35E+11	0.65	30856.0		
$bC_8H_{17}(+M) = yC_7H_{14} + CH_3(+M)$	LOW/1.58E+58	−12.85	35567.0/		D(1/4)
	TROE/0.986	−300	1	1E30/	
	2.14E+12	0.65	30856.0		
$bC_8H_{17}(+M) = oC7H_{14} + CH_3(+M)$	LOW/6.32E+58	−12.85	35567.0/		D
	TROE/0.986	−300	1	1E30/	
	1.07E+12	0.65	30856.0		
$dC_8H_{17}(+M) = pC_7H_{14} + CH_3(+M)$	LOW/3.16E+58	−12.85	35567.0/		D(1/2)
$xC_7H_{15}(+M) = dC_6H_{12} + CH_3(+M)$	TROE/0.986	−300	1	1E30/	
$dC_8H_{17}(+M) = C_3H_6 + neoC_5H_{11}(+M)$					
$dC_5H_{11}(+M) = C_2H_4 + iC_3H_7(+M)$	2.65E+13	0.00	27828.0		E(5/2)
$yC_7H_{15}(+M) = iC_3H_7 + iC_4H_8(+M)$	LOW/4.743E+55	−11.91	32263.0/		
$xC_7H_{15}(+M) = C_3H_6 + iC_4H_9(+M)$	TROE/0.987	−219.1	1 1E30/		
$dC_6H_{13}(+M) = iC_3H_7 + C_3H_6(+M)$					
	3.33E+13	0.00	3260.7		
$iC_8H_{16} + H(+M) = bC_8H_{17}(+M)$	LOW/1.565E+39	−6.66	7000.0/		F(5/2)
$jC_8H_{16} + H(+M) = dC_8H_{17}(+M)$	TROE/1.000	1000.0	1310.0	48097.0/	
$xC_7H_{14} + H(+M) = yC_7H_{15}(+M)$	1.45E+09	1.48	36010.0		
$cC_8H_{17}(+M) = jC_8H_{16} + H(+M)$	LOW/4.495E+56	−12.0	42170.0/		G(2/3)
	TROE/0.88	−1959	1	1E30/	
	2.18E+09	1.48	36010.0		
$xC_7H_{15}(+M) = xC_7H_{14} + H(+M)$	LOW/6.742E+56	−12.0	42170.0/		G
	TROE/0.88	−1959	1	1E30/	
	1.33E+13	0.00	1559.8		
$pC_7H_{14} + H(+M) = pC_7H_{15}(+M)$	LOW/8.70E+42	−7.50	4721.8/		H
$cC_6H_{12} + H(+M) = dC_6H_{13}(+M)$	TROE/1.000	1000.0	645.4	6844.3 /	
$nC_7H_{15} = aC_6H_{12} + CH3$	2.11E+24	−4.34	25145.0		I(2/3)
$neoC_5H_{11}(+M) = iC_4H_8 + CH3(+M)$	1.06E+13	0.00	27828.0		
$qC_7H_{15}(+M) = C_2H_4 + neoC_5H_{11}(+M)$	LOW/1.897E+55	−11.91	32263.0/		E
	TROE/0.987	−219.1	1	1E30 /	
$iC_8H_{16} + H(+M) = cC_8H_{17}(+M)$					
$yC_7H_{14} + H(+M) = yC_7H_{15}(+M)$					
$pC_7H_{14} + H(+M) = qC_7H_{15}(+M)$	1.33E+13	0.00	3260.7		
$dC_6H_{12} + H(+M) = dC_6H_{13}(+M)$	LOW/6.26E+38	−6.66	7000.0/		F
$neoC_6H_{12} + H(+M) = hC_6H_{13}(+M)$	TROE/1.000	1000.0	1310.0	48097.0/	
$cC_5H_{10} + H(+M) = dC_5H_{11}(+M)$					
$oC_7H_{14} + H(+M) = pC_7H_{15}(+M)$					

A $iC_4H_9 + H(+M) = iC_4H_{10}(+M)$ [41].
B $iC_3H_7 + H(+M) = C_3H_8(+M)$ [42].
C $tC_4H_9 + H(+M) = iC_4H_{10}(+M)$ [41].
D $iC_4H_9(+M) = C_3H_6 + CH_3(+M)$ [43].
E $pC_4H_9(+M) = C_2H_4 + C_2H_5(+M)$ [43].
F $C_3H_6 + H(+M) = nC_3H_7(+M)$ [44].
G $tC_4H_9(+M) = iC_4H_8 + H(+M)$ [45].
H $C_3H_6 + H(+M) = iC_3H_7(+M)$ [44].
I $neoC_5H_{11}(+M) = iC_4H_8 + CH_3(+M)$ (0.1 atm) [46].
[a] The value in the brackets is the revised coefficient of A factor.

to be reduced by 10 times. The sub-mechanism of *n*-heptane and iso-octane oxidation used in this study is the LLNL (Lawrence Livermore National Laboratory) PRF oxidation mechanism version 3, in which only *n*-heptane direct decomposition has been described as pressure dependent. Thus, the decomposition reactions of linear C7–C5 alkyl were adopted from JetSurF 2.0 [36]. Analogy method

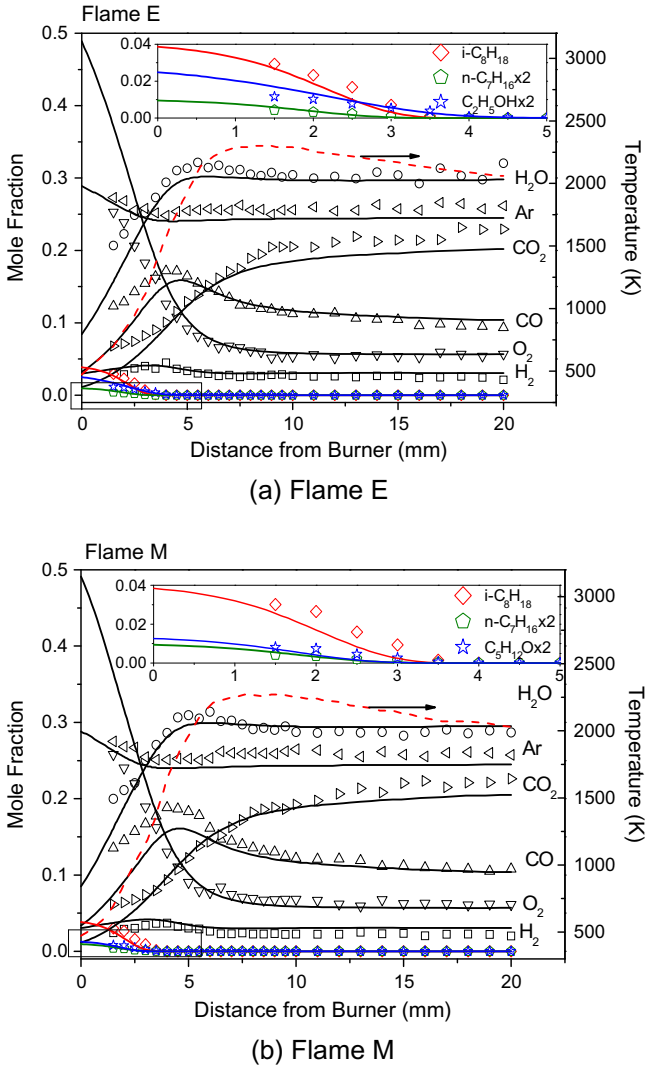

Fig. 1. Mole fractions of major species in Flame E and Flame M.

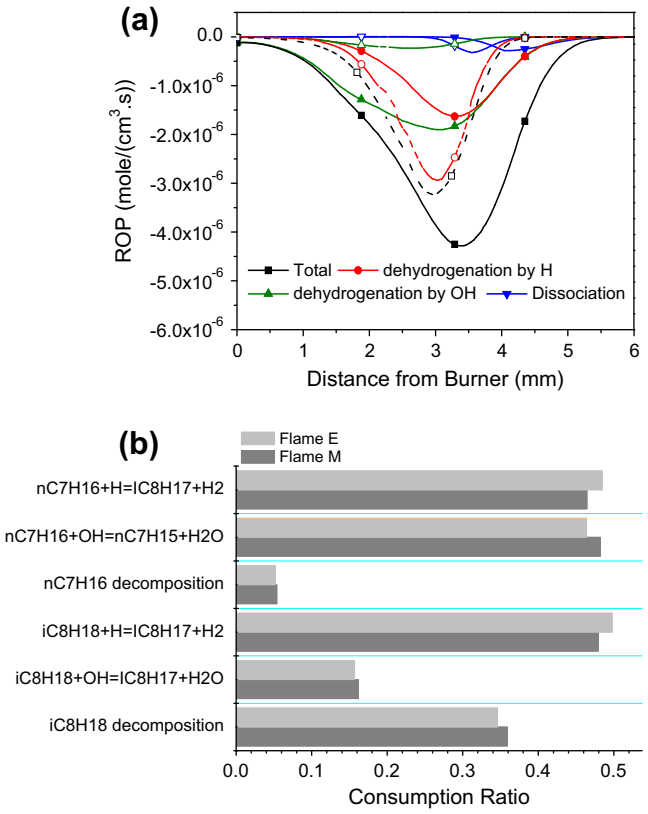

Fig. 2. ROP analysis of additives and distribution of consumption ratio for hydrocarbon fuels. (a) ROP analysis of ethanol and MTBE (the solid lines with solid symbols are the results of ethanol and the dash lines with open symbols are the results of MTBE). (b) Distribution of consumption ratio for *n*-heptane and iso-octane.

was used in rate coefficients revision for iso-octane related reactions. For example: the reaction rate constant of iso-octane decomposes into isooctyl and H is derived by the rate constant of isobutane decomposes into isobutyl and H. There are three "a carbons" and two "d carbons" in iso-octane (known from its structure $(CH_3)_3CCH_2CH(CH_3)_2$), so the rate coefficients of $aC_8H_{17} + H(+M) = iC_8H_{18}(+M)$ and $dC_8H_{17} + H(+M) = iC_8H_{18}(+M)$ are regarded to equal to that of $iC_4H_9 + H(+M) = iC_4H_{10}(+M)$ and 2/3 of it respectively. The important alkyl decomposition reactions in iso-octane reaction path were revised for pressure according to the similar method as well as the summaries described by Curran [37]. All the reactions using analogy amendment in rate coefficients revision are shown in Table 2. Comparative study before and after the analogy amendment for pressure was conducted for Flame E, as can be seen in Fig. S3 in Supplemental material. Overall, the mechanism with analogy amendment reproduces the experimental data better than the original mechanism for C_8H_{16}, C_7H_{14} and C_4H_8. These alkenes are contained in the revised reactions, but the predictions of other species are not improved further. Interaction reactions between one fuel molecule and the other fuel radical were also considered, because the interaction between fuel molecules exists mainly in those that have approximate molecular weights, such as *n*-heptane and iso-octane, according to literature [38]. We ensured that the adapted sub-mechanism can work well in other conditions from existed literatures, including a low-pressure laminar *n*-heptane flame ($\varphi = 0.94$) [39], a low-pressure laminar iso-octane flame ($\varphi = 0.94$) [39], a low-pressure laminar ethanol flame ($\varphi = 1.0$) [34] and a low-pressure flat MTBE flame ($\varphi = 0.18$) [15]. All of the validations of these flames can be seen in Figs. S4–S7 in Supplemental material. The adapted mechanism works reasonably well for all these flames. The present mechanism is not definitive but allows the discussion of some important findings that may be used in the further development of a more comprehensive and definitive model for the interaction between hydrocarbon fuels and oxygenated additives under a wide range of oxidation conditions. However, in the meantime, the multi-fuel oxidation mechanism is only applicable to the flames presented in this study. The PREMIX code combined with CHEMKIN was used in the numerical simulation [40]. The Soret effect and the multi-compound formulation were both under consideration. Given the nozzle effect in the flames, the temperature was decreased by a coefficient of 0.9, and the profiles were shifted away from the burner by 0.5 mm in the modeling. These revisions can yield more accurate position predictions for both the major species and the intermediates.

4. Results and discussion

4.1. Major species

Mole fractions of major species and temperature profiles are shown in Fig. 1. Generally, the modeling result fits the experimental data well. Species mole fractions have little difference between

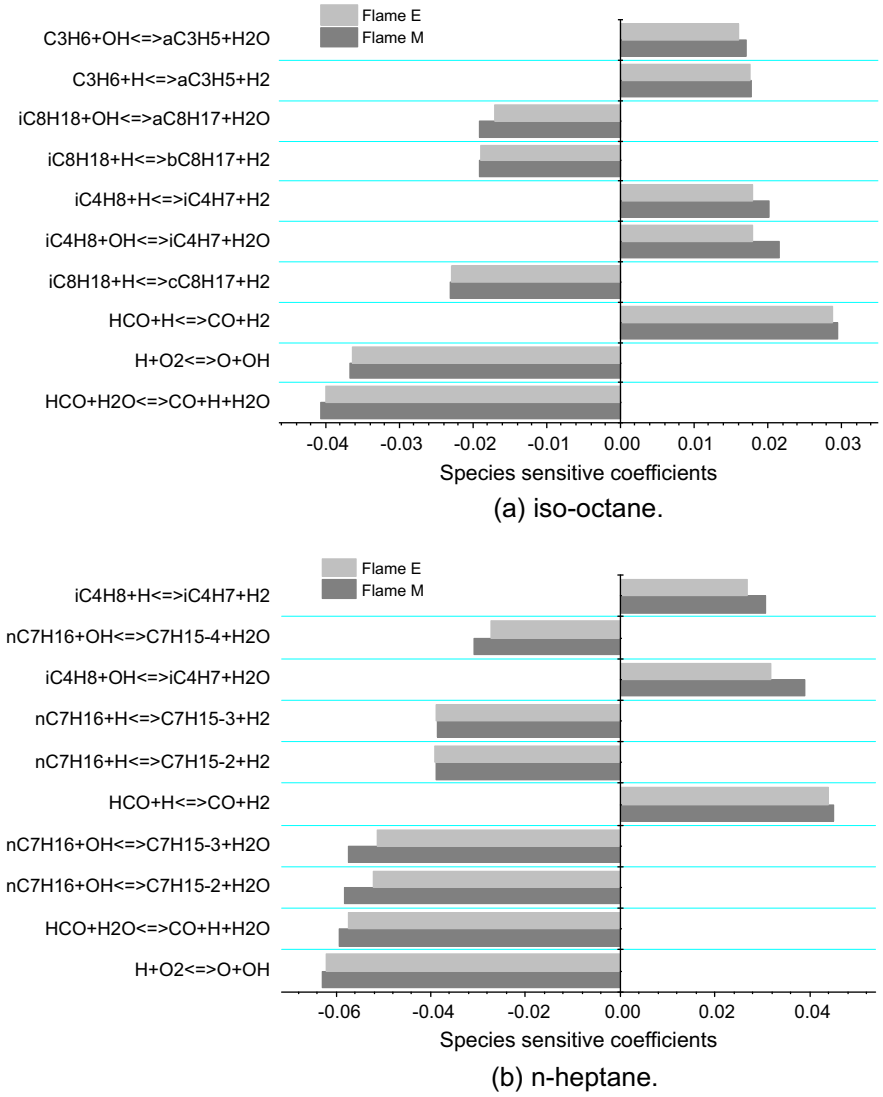

Fig. 3. Species sensitive coefficients of iso-octane and *n*-heptane.

two flames in most zones. The almost same temperatures of two flames provide the similar flame structures and reaction atmosphere, which is beneficial for their comparison. The difference exists only in the reaction zone. As the ROP (rate of production) analysis shows in Fig. 2a, the consumption paths of ethanol and MTBE are different. The strong reaction activity of ethanol is primarily shown at low-temperature zone while relatively weakens at high-temperature zone. MTBE has totally high reaction rate once the reactants enter high temperature zone, and the burn out position of MTBE (about 4.0 mm) is much ahead of that of ethanol (about 5.5 mm). The main difference exists in the dehydrogenation by small radicals: most MTBE goes H path while most ethanol goes both OH and H paths. MTBE dehydrogenation by H is violent at high temperature because massive H radical is produced only at high temperature through $CO + OH = CO_2 + H$, and its direct decomposition also has lower activation energy. Mole fractions of iso-octane and *n*-heptane show no apparent difference with the oxygenated additive changed. So the consumption distribution ratio analysis of iso-octane and *n*-heptane is conducted, as shown in Fig. 2b. It can be seen that iso-octane is mainly consumed by dehydrogenation and decomposition while *n*-heptane is consumed only by dehydrogenation. All ratio bars between iso-octane and *n*-heptane have the differences within 3% no matter what additive is used. Flame M has lower values for reactions involving H atom but higher values for reactions involving OH radical. The participation of more H atom and less OH radical in MTBE dehydrogenation than in ethanol should be a reasonable explanation for this difference.

Species sensitive analysis, which is another kinetic analysis method, is used in this study to compare differences of critical reactions between the two flames. Fig. 3 shows sensitive coefficients of hydrocarbon fuels of top 10 reactions at the height of 2.0 mm above the burner. The positive value of the coefficient indicates the reaction has a negative effect on the species consumption. Coefficients of most reactions have little change with the change of additives. The change of fuel dehydrogenation sensitivities has the same trend with the distribution ratio shown in Fig. 2a. That is Flame M has higher distribution ratio of dehydrogenation by OH radical and the correspondingly higher sensitivity for reactions involving OH radicals. *N*-heptane is more sensitive to the change of additives than iso-octane is (shown in Fig. 2b), because the consumption of *n*-heptane highly depends on H-abstraction by radicals rather than by direct decomposition. Reactions involving iso-butene (iC_4H_8) are another change for both iso-octane and *n*-heptane. Coefficients of $iC_4H_8 + OH \Longleftrightarrow iC_4H_7 + H_2O$ and $iC_4H_8 + H \Longleftrightarrow iC_4H_7 + H_2$, which are important reactions relating

to the radical elimination, increase by about 15.58%, and 9.92% for iso-octane and 17.40% and 11.20% for *n*-heptane respectively when ethanol is changed to MTBE. This behavior suggests the increase of iso-butene is due to the MTBE addition.

4.2. Intermediates

4.2.1. Alkenes

Alkenes detected from two flames are shown in Fig. 4. The mole fraction of each alkene is the sum of its isomers. Both the experiment and modeling results show that the mole fraction of heptene (C_7H_{14}) has the largest value. The mole fraction profiles of C5–C8 alkenes, which come from unimolecular decomposition of alkyl especially heptyl and octyl, have no significant difference in two flames. This indicates that the initial dehydrogenation and decomposition of hydrocarbon fuels are not affected by ethanol or MTBE addition. Iso-butene has a sensible difference in two flames. Iso-butene is a typical product of iso-octane decomposition, and most of it is produced by following paths: $C_8H_{18} \rightarrow C_8H_{17} \rightarrow iC_4H_8$ (the second stage takes 46.20% and 46.13% of C_8H_{17} consumption in Flame E and Flame M respectively). Iso-butene is also a critical product of MTBE degeneration: for instance, $MTBE \rightarrow iC_4H_8OCH_3 \rightarrow iC_4H_8$ (the first stage takes 20.84% of MTBE consumption). Considering the same quantity of iso-octane in the flames, the addition of MTBE leads to the increase of iso-butene in Flame M.

Propene (C_3H_6) and ketene (C_2H_2O) cannot be separated easily since they have nearly the same molecular weight and ionization energy, and their PICSs are almost the same at 10 eV (7.01 for ketene and 7.05 for propene), which allows them to be treated as one species. The profile shows mainly propene mole fraction, because the modeling result shows that the amount of ketene is two orders of magnitude less than propene. The mole fractions in two flames are more or less the same. Propene is mainly produced through $aC_3H_5 + H(+M) = C_3H_6(+M)$ (32.00% in Flame E and 31.36% in Flame M), and $iC_4H_8 + H = C_3H_6 + CH_3$ (25.28% in Flame E and 26.87% in Flame M).

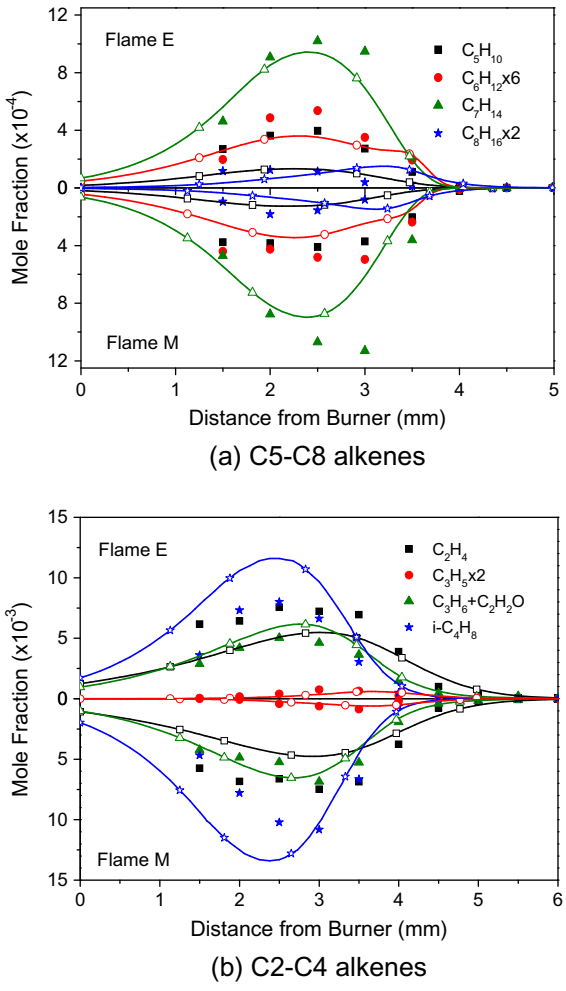

Fig. 4. Mole fractions of alkenes in two flames (the solid symbols are experiment results, the dashed lines with open symbols are modeling results, the same below).

Ethylene (C_2H_4) shows no difference between two flames. For hydrocarbon fuels, ethylene comes mainly from alkyl decomposition or H addition of alkenes to alkyl radical and subsequent decomposition. For the additives, both MTBE and ethanol have ethylene production paths. MTBE has the alkyl decomposition while ethanol has the fuel dehydrogenation (35.30% of ethanol is consumed through $C_2H_5OH + X = C_2H_4OH + HX$) and decomposition (12.31% of C_2H_4 is produced by $C_2H_4OH = C_2H_4 + OH$) paths.

4.2.2. Other hydrocarbons

Other hydrocarbons detected in two flames are shown in Fig. 5. Fig. 5a illustrates alkanes and alkyl radicals. Propane and butane are also detected, but they are not considered in the mole fraction deducing since their weak signals in the mass spectra are covered by acetaldehyde and acetone, which have close molecular weights with propane and butane respectively but strong signals. Mole fraction profiles of alkanes, which are by-products in two flames and come mainly from H addition to alkyl radical, nearly show no difference between the two flames. Methyl (CH_3) is a common degeneration product of all fuels consider in this study, its mole fraction profiles are more or less the same in two flames.

Alkadienes are shown in Fig. 5b. Generally, more alkadienes are produced in Flame M, similar to butane (shown in Fig. 4b). Alkadienes come mainly from alkenes dehydrogenation. Taking allene (aC_3H_4) for example, its production paths are [47]: 1. Combination of small molecule hydrocarbons such as $CH_2 + C_2H_2 = CH_2CCH_2$; 2. Dehydrogenation of straight-chain alkenes: $CH_2CHCH_3 \rightarrow CH_2CHCH_2 \rightarrow CH_2CCH_2$; 3. Branch-chain alkenes' dehydrogenation and separation of the C–C bond: $iC_4H_8 \rightarrow iC_4H_7 \rightarrow CH_2CCH_2 + CH_3$. Path 3 is the major path of aC_3H_4 production, as $iC_4H_7 = CH_2CCH_2 + CH_3$ takes 42.71% and 45.04% of its production, path 2 takes 32.38% and 30.91%, and path 1 takes 2.73% and 2.23% in Flame E and Flame M, respectively. The slight higher quantity of aC_3H_4 in Flame M is caused by the higher iC_4H_8 in Flame M. 1,3-butadiene (C_4H_6) is also mainly produced through path 3: $C_4H_7 \Longleftrightarrow C_4H_6 + H$ takes 74.00% of C_4H_6 production in Flame E and 74.67% in Flame M.

Alkynes are illustrated in Fig. 5c. Most alkynes come from dehydrogenation of alkenes. Mole fractions of alkynes in Flame M are almost the same as those in Flame E. Propyne (pC_3H_4), which is the isomer of allene, shows less difference in two flames unlike the perceived differences of alkadienes, iso-butene and propene. This indicates alkynes have lower sensitivity to the change of additives than alkadienes do, the potential reason is their chemical stability is driven by their low Gibbs free energy at high temperature.

Alkenynes are further dehydrogenation products of alkadienes and alkynes and also could be polymerization products of small molecule unsaturated hydrocarbons. As can be seen from Fig. 5d, their mole fraction profiles in two flames have little difference, indicating the influence of different additives does not spread to species with high unsaturation degree. Benzene is the only aromatic found in this study. Benzene formation in two flames is mainly through C3 + C3 path (40.62% in Flame M and 37.84% in Flame E) and C2 + C4 path (21.48% in Flame M and 24.66% in Flame E). Because the difference of major benzene precursors (C_2H_2, C_3H_3, and C_4H_4) between the two flames cannot be distinguished, the similar profiles of benzene presented in two flames are reasonable.

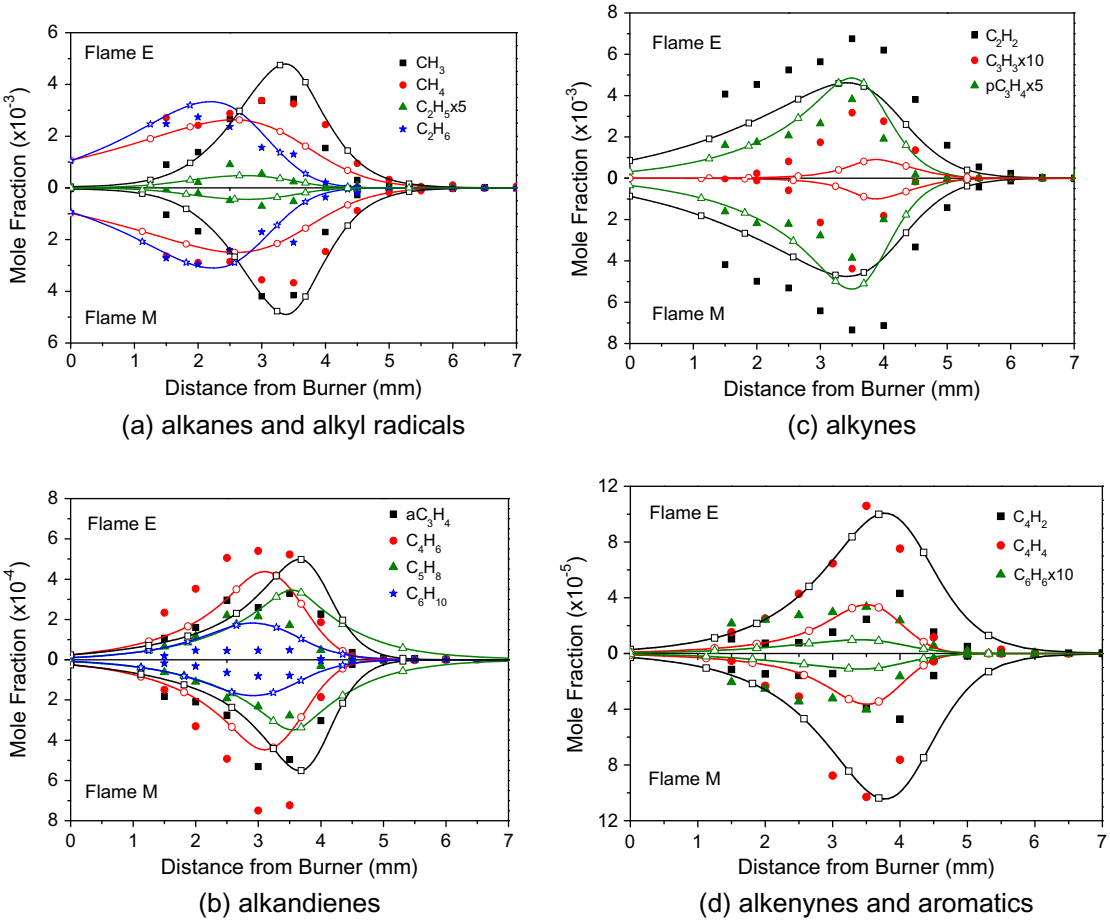

Fig. 5. Mole fractions of other hydrocarbons in two flames.

4.2.3. Oxygenated intermediate products

Methanol is the only alcohol detected in two flames except ethanol fuel. The amount of methanol in Flame M is about 50% higher than that in Flame E in the experiment while almost the same in the modeling result, shown in Fig. 6a. The main methanol production paths are $CH_3O \rightarrow CH_3OH$ (50.93% in Flame M and 61.66% in Flame E) and $OH + CH_3(+M) \Longleftrightarrow CH_3OH(+M)$ (35.83% in Flame M and 33.67% in Flame E), while there is another path in Flame M: $MTBE(+M) \Longleftrightarrow iC_4H_8 + CH_3OH(+M)$ (8.28%).

Flame M has slightly higher formaldehyde but much lower acetaldehyde (about 1/3 of that in Flame E, shown in Fig. 6a). Most formaldehyde in two flames is the species produced in the final stage ($CH_2O \rightarrow HCO \rightarrow CO \rightarrow CO_2$) of the two hydrocarbon fuels oxidation. For the two additives, there exists formaldehyde production shortcuts: $C_2H_5OH \rightarrow CH_3CH_2O \rightarrow CH_2O$ takes 2.30% of formaldehyde production in Flame E; $MTBE \rightarrow (CH_3)_3COCH_2 \rightarrow CH_2O$ takes 5.83% in Flame M. Acetaldehyde, also one of the post-oxidation products in hydrocarbon fuel flames, is higher in Flame E because it can be produced by ethanol dehydrogenation through: $C_2H_5OH \rightarrow CH_3CHOH/CH_3CH_2O \rightarrow CH_3CHO$, which takes 77.85% of its production. There are other reactions in both flames: $iC_3H_7 \rightarrow CH_3CHO$ (10.90% in Flame E and 36.98% in Flame M), $C_2H_5 + O = CH_3CHO + H$ (5.53% in Flame E and 17.23% in Flame M).

Carbonyl compounds including ketene and up to C5 carbonyl compounds are detected in two flames, as shown in Fig. 6b. Acetone (C_3H_6O) and butanone (C_4H_8O) show visible differences. Acetone and butanone are mainly produced directly from reactions: $tC_4H_9 \rightarrow C_3H_6O$ and $tC_4H_9 \rightarrow iC_4H_8O$. Mole fractions of C3 and C4 carbonyl compounds in Flame M are a little higher, because tC_4H_9 is a major degeneration product of MTBE. Modeling results of these species were not shown in the figure because their generation and consumption should involve low temperature oxidation reactions which are not considered comprehensively in current mechanism.

5. Conclusions

Species in premixed laminar PFR90/ethanol and PRF90/MTBE flames with the same blending ratio were investigated quantitatively using molecular beam sampling technology combining with tunable synchrotron VUV photoionization mass spectrometry under 25 torr. A mechanism for multi-fuels high temperature oxidation under low pressure was developed and modeling study with satisfied prediction was conducted for kinetic analysis. The main conclusions are summarized as follows:

1. The structures of the flames with different oxygenated additives are almost the same. There are differences between consumption paths of ethanol and MTBE: ethanol is mainly consumed through H abstraction by OH and H, while MTBE is mainly consumed through dehydrogenation by H atom at high temperature. This difference leads to the slight change of radical pool, and the consumption paths and species sensitive coefficients of hydrocarbon fuels.
2. Both experimental and modeling results show that mole fractions of iso-butene, 1,3-butadiene and allene are higher in Flame M than those in Flame E. However, further dehydrogenation or polymerization products with high unsaturation degree are not affected.

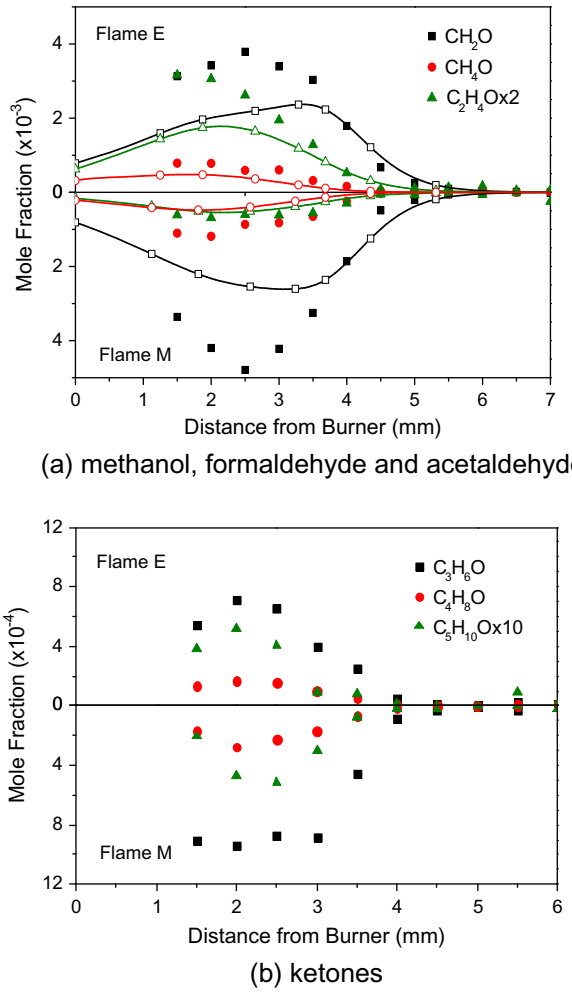

Fig. 6. Mole fractions of oxygenated intermediates in two flames.

3. Both experimental and modeling results show that the mole fraction of the acetaldehyde has higher level in Flame E, while the experimental result shows that mole fractions of formaldehyde, methanol, acetone and butanone have higher level in Flame M. Other species not mentioned are not affected by the change of additive.

Acknowledgements

The authors acknowledge the financial support by the Natural Science Foundation of China (No. 51176135) and National High-tech R&D Project (863 Program) (No. 2012AA111719) of the Ministry of Science and Technology of China. And the authors also thank Professor Fei Qi and his team in National Synchrotron Radiation Laboratory of China for their assistance in the flame experiment.

Appendix A. Supplementary material

Supplementary data associated with this article can be found, in the online version, at http://dx.doi.org/10.1016/j.fuel.2013.04.038.

References

[1] Braids OC. Commentaries and perspectives MTBE-panacea problem. Environ Forensics 2001;2(3):189–96.
[2] Poulopoulos S, Philippopoulos C. Influence of MTBE addition into gasoline on automotive exhaust emissions. Atmos Environ 2000;34(28):4781–6.
[3] Hamai K, Mitsumoto H, Iwakiri Y, Ishihara K, Ishii M. Effects of clean fuels (reformulated gasolines, M85, and CNG) on automotive emissions. SAE technical paper: 922380; 1992.
[4] Hasan MA. Effect of ethanol–unleaded gasoline blends on engine performance and exhaust emission. Energy Convers Manage 2003;44(9):1547–61.
[5] Niven RK. Ethanol in gasoline: environmental impacts and sustainability review article. Renew Sust Energy Rev 2005;9(6):535–55.
[6] Yüksel F, Yüksel B. The use of ethanol–gasoline blend as a fuel in an SI engine. Renew Energy 2004;29(7):1181–91.
[7] Koç M, Sekmen Y, Topgül T, Yücesu HS. The effects of ethanol–unleaded gasoline blends on engine performance and exhaust emissions in a spark-ignition engine. Renew Energy 2009;34(10):2101–6.
[8] Hsieh WD, Chen RH, Wu TL, Lin TH. Engine performance and pollutant emission of an SI engine using ethanol–gasoline blended fuels. Atmos Environ 2002;36(3):403–10.
[9] Ceviz MA, Yüksel F. Effects of ethanol–unleaded gasoline blends on cyclic variability and emissions in an SI engine. Appl Therm Eng 2005;25(5–6):917–25.
[10] Franklin PM, Koshland CP, Lucas D, Sawyer RF. Evaluation of combustion by-products of MTBE as a component of reformulated gasoline. Chemosphere 2001;42(5–7):861–72.
[11] Poulopoulos SG, Samaras DP, Philippopoulos CJ. Regulated and unregulated emissions from an internal combustion engine operating on ethanol-containing fuels. Atmos Environ 2001;35(26):4399–406.
[12] Song CL, Zhang WM, Pei YQ, Fan GL, Xu GP. Comparative effects of MTBE and ethanol additions into gasoline on exhaust emissions. Atmos Environ 2006;40:1957–70.
[13] Leplat N, Dagaut P, Togbé C, Vandooren J. Numerical and experimental study of ethanol combustion and oxidation in laminar premixed flames and in jet-stirred reactor. Combust Flame 2011;158(4):705–25.
[14] Saxena P, Williams FA. Numerical and experimental studies of ethanol flames. Proc Combust Inst 2007;31(1):1149–56.
[15] Van Der Loos A, Vandooren J, Van Tiggelen PJ. Kinetic study of methyl tert-butyl ether (MTBE) oxidation in flames. In: International symposium on combustion 1998;27(1):477–84.
[16] Brocard JC, Baronnet F, O'Neal HE. Chemical kinetics of the oxidation of methyl tert-butyl ether (MTBE). Combust Flame 1983;52:25–35.
[17] Dagaut P, Togbé C. Experimental and modeling study of the kinetics of oxidation of ethanol-*n*-heptane mixtures in a jet-stirred reactor. Fuel 2010;89(2):280–6.
[18] Haas FM, Chaos M, Dryer FL. Low and intermediate temperature oxidation of ethanol and ethanol-PRF blends: an experimental and modeling study. Combust Flame 2009;156:2346–50.
[19] Song JO, Yao CD, Liu SY, Xu HJ. Effects of ethanol addition on *n*-heptane decomposition in premixed flames. Energy Fuels 2008;22(6):3806–9.
[20] Song JO, Yao CD, Liu SY, Tian ZY, Wang J. Experiment study of oxygenates impact on *n*-heptane flames with tunable synchrotron vacuum UV photoionization. Fuel 2009;88(11):2297–302.
[21] Yao CD, Yang XL, Raine RR, Cheng CH, Tian ZY, Li YY. The effects of MTBE/ethanol additives on toxic species concentration in gasoline flame. Energy Fuels 2009;23(7):3543–8.
[22] Yao CD, Li J, Li Q, Huang CQ, Wei LX, Wang J, et al. Study on combustion of gasoline/MTBE in laminar flame with synchrotron radiation. Chemosphere 2007;67(10):2065–71.
[23] Cool TA, McIlroy A, Qi F, Westmoreland PR, Poisson L, Peterka DS, et al. Photoionization mass spectrometer for studies of flame chemistry with a synchrotron light source. Rev Sci Instrum 2005;76:094–102.
[24] Hansen N, Cool TA, Westmoreland PR, Kohse-Höinghaus K. Recent contributions of flame-sampling molecular-beam mass spectrometry to a fundamental understanding of combustion chemistry. Prog Energy Combust 2009;35(2):168–91.
[25] Qi F, Yang R, Yang B, Huang CQ, Wei LX, Wang J, et al. Isomeric identification of polycyclic aromatic hydrocarbons formed in combustion with tunable vacuum ultraviolet photoionization. Rev Sci Instrum 2006;77(8):084101.
[26] Cool TA, Nakajima K, Taatjes CA, McIlroy A, Westmoreland PR, Law ME, et al. Studies of a fuel-rich propane flame with photoionization mass spectrometry. Proc Combust Inst 2005;30(1):1681–8.
[27] Cool TA, Wang J, Hansen N, Westmoreland PR, Dryer FL, Zhao Z, et al. Photoionization mass spectrometry and modeling studies of the chemistry of fuel-rich dimethyl ether flames. Proc Combust Inst 2007;31(1):285–93.
[28] Photonionization Cross Section Database (Version 1.0). Hefei, China: National Synchrotron Radiation Laboratory; 2011. <http://flame.nsrl.ustc.edu.cn/en/database.htm>.
[29] Koizumi H. Predominant decay channel for superexcited organic molecules. J Chem Phys 1991;95(8):5846–52.
[30] Kint JH. A noncatalytic coating for platinum–rhodium thermocouples. Combust Flame 1970;14(2):279–81.
[31] Fristrom RM. Flame structure and processes. New York: Oxford; 1995.
[32] Hartlieb AT, Atakan B, Kohse-Höinghaus K. Effects of a sampling quartz nozzle on the flame structure of a fuel-rich low-pressure propene flame. Combust Flame 2000;121(4):610–24.
[33] Li J. Experimental and numerical studies of ethanol chemical kinetics. Ph D thesis. Princeton University; 2005.
[34] Xu HJ, Yao CD, Yuan T, Zhang KW, Guo HJ. Measurements and modeling study of intermediates in ethanol and dimethy ether low-pressure premixed flames using synchrotron photoionization. Combust Flame 2011;158(9):1673–81.

[35] Yasunaga K, Simmie JM, Curran HJ, Koike T, Takahashi O, Kuraguchi Y, et al. Detailed chemical kinetic mechanisms of ethyl methyl, methyl tert-butyl and ethyl tert-butyl ethers: the importance of uni-molecular elimination reactions. Combust Flame 2011;158(6):1032–6.
[36] Wang H, Dames E, Sirjean B, Sheen DA, Tangko R, Violi A, et al. A high-temperature chemical kinetic model of *n*-alkane (up to *n*-dodecane), cyclohexane, and methyl-, ethyl-, *n*-propyl and *n*-butyl-cyclohexane oxidation at high temperatures. JetSurF version 2.0, September 19; 2010. <http://melchior.usc.edu/JetSurF/JetSurF2.0>.
[37] Curran HJ. Rate constant estimation for C1 to C4 alkyl and alkoxyl radical decomposition. Int J Chem Kinet 2006;38(4):250–75.
[38] Andrae J, Johansson D, Björnbom P, Risberg P, Kalghatgi G. Co-oxidation in the auto-ignition of primary reference fuels and *n*-heptane/toluene blends. Combust Flame 2005;140(4):267–86.
[39] Yuan T. Experimental and kinetic modeling studies on pyrolysis and premixed flame of *n*-heptane and iso-octane. Ph D thesis. University of Science and Technology of China; 2010.
[40] Kee RJ, Grcar JF, Smooke MD, Miller JA. Sandia, Report, SAND85-8240; 1985.
[41] Tsang W. Chemical kinetic data base for combustion chemistry. Part 4. Isobutane. J Phys Chem Ref Data 1990;19(1):1–68.
[42] Tsang W. Chemical kinetic data base for combustion chemistry. Part 3. Propane. J Phys Chem Ref Data 1988;17:887.
[43] Knyazev VD, Slagle IR. Unimolecular decomposition of *n*-C4H9 and iso-C4H9 radicals. J Phys Chem 1996;100(13):5318–28.
[44] Tsang W. Chemical kinetic data base for combustion chemistry. Part V. Propene. J Phys Chem Ref Data 1991;20:221.
[45] Knyazev VD, Dubinsky IA, Slagle IR, Gutman D. Unimolecular decomposition of T-C4h9 radical. J Phys Chem 1994;98(20):5279–89.
[46] Slagle IR, Batt L, Gmurczyk GW, Gutman D, Tsang W. Unimolecular decomposition of the neopentyl radical. J Phys Chem 1991;95(20):7732–9.
[47] McEnally CS, Ciuparu DM, Pfefferle LD. Experimental study of fuel decomposition and hydrocarbon growth processes for practical fuel components: heptanes. Combust Flame 2003;134(4):339–53.